Dependence of dislocation damping on helium-3 concentration in helium-4 crystals



2014 J. Phys.: Conf. Ser. 568 012003

(http://iopscience.iop.org/1742-6596/568/1/012003)

Journal of Physics: Conference Series **568** (2014) 012003 doi:10.1088/1742-6596/568/1/012003

# Dependence of dislocation damping on helium-3 concentration in helium-4 crystals

**A D Fefferman,[1,*] F Souris,[1,*] A Haziot,[1,2] J R Beamish[1,3] and S Balibar[1]**

[1] Laboratoire de Physique Statistique de l'ENS, associé au CNRS et aux Universités D. Diderot et P.M. Curie, 24 rue Lhomond 75231 Paris Cedex 05, France
[2] Present Address: Department of Physics, The Pennsylvania State University, University Park, Pennsylvania 16802, USA
[3] Department of Physics, University of Alberta, Edmonton, Alberta, Canada T6G 2E1
[*] These authors contributed equally.

E-mail: balibar@lps.ens.fr

**Abstract.** The mechanical properties of crystals are strongly affected by dislocation mobility. Impurities can bind to dislocations and interfere with their motion, causing changes in the crystal's shear modulus and mechanical dissipation. In $^4$He crystals, the only impurities are $^3$He atoms, and they can move through the crystal at arbitrarily low temperatures by quantum tunneling. When dislocations in $^4$He vibrate at speeds $v < 45$ $\mu$m/sec, bound $^3$He impurities move with the dislocations and exert a damping force $B_3 v$ on them. In order to characterize $^4$He dislocation networks and determine the $^3$He binding energy, it is usually assumed that $B_3$ is proportional to the concentration of $^3$He bound to the dislocations. In this preliminary report, we determine $B_3$ in a crystal with 2.32 ppm $^3$He and compare with our previous measurements of $B_3$ in natural purity $^4$He crystals to verify the assumption of proportionality.

## 1. Introduction

Recent work[1, 2, 3, 4, 5] has demonstrated that the mechanical properties of hcp $^4$He crystals can be understood in great detail by modeling their dislocations as elastic strings that vibrate between pinning points[6]. At low dislocation speeds and low temperatures, $^3$He impurities bind to the dislocations and move with them, damping their vibrations[3]. The binding energy $E_B$ was determined from the frequency dependence of the peak dissipation temperature under the assumption that the damping due to $^3$He is proportional to the concentration of $^3$He atoms bound to the dislocations [3, 5, 7]. In order to test this assumption, we are measuring the $^3$He damping coefficient as a function of the $^3$He concentration in the helium gas that we use to grow our crystals. In this preliminary paper, we report the $^3$He damping coefficient for a crystal with a 2.32 ppm bulk $^3$He concentration and compare with that of crystals made of natural purity helium. We find a linear dependence on $^3$He concentration.

Dislocations in $^4$He crystals are strongly pinned where they intersect, forming a network characterized by an average length $L_N$ between network nodes and a density $\Lambda$ that is given by the total dislocation length per unit volume of the crystal. In the absence of damping, the dislocations vibrate elastically between pinning points in response to an oscillating stress. (No effect of the lattice potential on dislocation vibrations has been detected in hcp $^4$He [1].) This

results in a strain $\epsilon_{\rm dis}$ that adds to the strain $\epsilon_{\rm el}$ for the case of immobile dislocations [8]. The additional strain $\epsilon_{\rm dis}$ causes the shear modulus $\mu$ to decrease from the intrinsic value $\mu_{\rm el}$:

$$\mu = \frac{\mu_{\rm el}}{1 + \epsilon_{\rm dis}/\epsilon_{\rm el}}. \tag{1}$$

The magnitude of the softening $(\mu_{\rm el} - \mu)/\mu_{\rm el}$ is of order 1 with mobile dislocations, but it is reduced by damping of dislocation motion by bound $^3$He impurities or thermal phonons. We define a relaxation time $\tau = BL_N^2/\pi^2 C$, where $B$ is the damping coefficient, $C = \mu_{\rm el} b^2 \ln(R/r)/[4\pi(1-\nu)] = 2.3 \times 10^{-12}$ N is the tension in the dislocation line, $b = 0.367$ nm is the Burgers vector, $\nu = 0.33$ is Poisson's ratio, $R \approx L_N \approx 100$ $\mu$m is the typical spacing between dislocations, and $r \approx 1$ nm is the diameter of the dislocation core [9]. For the case of a constant $L_N$ (i.e. no pinning by bound $^3$He), we have[5]

$$\frac{\epsilon_{\rm dis}}{\epsilon_{\rm el}} = \alpha \Lambda L_N^2 \frac{1 - i\omega\tau}{1 + (\omega\tau)^2} \tag{2}$$

where $\omega/2\pi$ is the driving frequency, $\alpha = 32\,(1-\nu)\,/\pi^4 \ln(R/r) = 0.019$. Equations 1 and 2 show that as $B$ increases, $\mu$ increases to its intrinsic value $\mu_{\rm el}$ and the dissipation $Q^{-1} = {\rm Im}[\mu]\,/{\rm Re}[\mu]$ passes through a maximum at $\omega\tau = \sqrt{1 + \alpha\Lambda L_N^2}$ [5]. We use Eqs. 1 and 2 along with measurements in the phonon damping regime to determine $\Lambda$ and $L_N$ for a given crystal [2], and then use Eqs. 1 and 2 along with measurements on the same crystal in the $^3$He damping regime to determine the $^3$He damping coefficient.

## 2. Experimental details

Our crystal growth and shear modulus measurement techniques have been explained in detail in previous publications [1, 5]. Inside the measurement cell, two piezoelectric shear plates face each other with a separation of 0.7 mm, forming a narrow gap that is filled with an oriented $^4$He crystal (Fig. 1 inset). The orientation of the crystal is determined by photographing its growth shape through the windows of the cryostat at constant temperature and pressure. Applying a voltage $V$ to one transducer produces a shear strain $\epsilon = V d_{15}$ in the $^4$He crystal, where $d_{15} = 95$ pm/V below 1 K [1]. The resulting stress $\sigma$ in the $^4$He is measured with the opposite transducer. The shear modulus is then given by $\mu = \sigma/\epsilon$. The present measurements were of a crystal with 2.32 ppm $^3$He concentration that was oriented so that its six-fold axis of symmetry was nearly aligned with motion of the drive transducer, with spherical coordinates $\theta = 1.93$ deg and $\phi = 52.1$ deg, where $\theta$ is the polar coordinate measured relative to $z$ and $\phi$ is the azimuthal coordinate measured relative to $x$ (coordinates defined in Fig. 1 inset). As a result, the maximum shear modulus $\mu_{\rm el}$ for this orientation was within 1 % of the intrinsic value at melting pressure of the elastic coefficient $c_{44} = 124$ bar [1, 10]. The crystal was grown at 1.4 K so that any small liquid droplets that could trap $^3$He solidified as the crystal was cooled below 1 K.

## 3. Results and discussion

We used high drive, high frequency measurements to determine $L_N$ and $\Lambda$ for our crystal ($x_3 = 2.32$ ppm), as in [2]. Figure 1 shows the dissipation and shear modulus measured on cooling at a driving frequency of $\omega/2\pi = 16$ kHz and a rms driving strain $\epsilon = 2.3 \times 10^{-6}$. The shear modulus decreased monotonically while cooling because the high $\epsilon$ prevented $^3$He atoms from binding to the dislocations, except at the very lowest temperatures where a small amount of binding occurred. At the same time, this driving strain is low enough to prevent irreversible deformation of the crystal. The overlap of the three different measurements in Fig. 1, which were made on different days, demonstrates the high degree of reproducibility of the measurement.

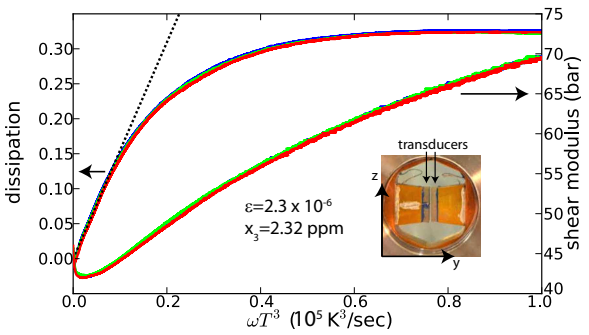


**Figure 1.** Solid curves: The dissipation and shear modulus measured on cooling at a driving frequency of $\omega/2\pi = 16$ kHz and a rms driving strain of $2.3 \times 10^{-6}$. The $^3$He concentration was 2.32 ppm. The different colors correspond to measurements on different days, which demonstrate excellent reproducibility. The dashed line demonstrates the linear dependence of $Q^{-1}$ on $\omega T^3$ in the limit of low $T$, as predicted by Eq. 4, which allows us to determine the average network length $L_N = 158$ $\mu$m and dislocation density $\Lambda = 4.1 \times 10^5/\text{cm}^2$. Inset: The experimental cell used for these measurements (see text).

Since $^3$He atoms were not binding to the dislocations in these high drive measurements, thermal phonons made the only contribution to the dislocation damping. It was shown in [2] that thermal phonons damp dislocations by the fluttering mechanism in this temperature range, so that the damping coefficient is $B_{\text{ph}} = 14.4 k_B^3 T^3/\pi^2\hbar^2 c^3 \approx 2.1 \times 10^{-8}\ T^3$ Pa s where $c$ is the sound speed [11, 12], and the relaxation time is $\tau_{\text{ph}} = B_{\text{ph}} L_N^2/\pi^2 C$. Substituting $\tau_{\text{ph}}$ for $\tau$ in Eq. 2 and using Eq. 1 yields, at low temperatures where the phonon damping is small, a maximum softening

$$\frac{\Delta\mu}{\mu_{\text{el}}} \equiv \frac{\mu_{\text{el}} - \mu}{\mu_{\text{el}}} = \frac{\alpha\Lambda L_N^2}{1 + \alpha\Lambda L_N^2} \tag{3}$$

and a dissipation

$$Q^{-1} = \frac{\Delta\mu}{\mu_{\text{el}}}\omega\tau_{\text{ph}} = \frac{\Delta\mu}{\mu_{\text{el}}}\frac{14.4 k_B^3}{\pi^4\hbar^2 c^3}\frac{L_N^2}{C}\omega T^3. \tag{4}$$

The dashed line in Fig. 1 shows that $Q^{-1}$ has a linear dependence on $\omega T^3$, as predicted by Eq. 4. Thus we substitute the maximum softening $\Delta\mu/\mu_{\text{el}} = 0.664$ and the low temperature slope $Q^{-1}/\omega T^3 = 1.55 \times 10^{-5}$ sec/K$^3$ from Fig. 1 into Eqs. 3 and 4 to determine $L_N = 158$ $\mu$m and $\Lambda = 4.1 \times 10^5/\text{cm}^2$.

Having characterized the dislocation network, we can now determine the $^3$He damping coefficient. We used measurements at low drive and low frequency, and thus low dislocation speed, for this purpose. Figure 2 shows the temperature dependence of $\mu$ and $Q^{-1}$ in this limit, measured on cooling with the same crystal as in Fig. 1. The shear modulus increases monotonically as the crystal is cooled because $^3$He atoms progressively bind to the dislocations and damp their motion. Because the measurements in Fig. 2 are at low frequency, damping by thermal phonons is now negligible. At the lowest temperatures, $\mu = \mu_{\text{el}}$. Near the midpoint of the temperature variation of $\mu$ at each frequency, $Q^{-1}$ reaches a maximum at a temperature $T_p$.

The black circles in Fig. 3 show $1/T_p$ measured in the 2.32 ppm crystal at different driving frequencies, including the measurements shown in Fig. 2. We can derive an expression for the frequency dependence of $T_p$ by initially assuming that the $^3$He damping coefficient $B_3$ scales with some power $n$ of $x_d$, the concentration of bound $^3$He, i.e., $B_3 = B_0 x_d^n$, where $x_d = x_3 \exp(E_B/T)$ and $x_3$ is the bulk $^3$He concentration. We will determine $B_0 x_3^n$ from our fit (in previous work [7, 3, 5], it was assumed that $n = 1$). Equations 1 and 2 imply that the dissipation attains a maximum value at the temperature $T_p$ at which $\omega\tau = \sqrt{1 + \alpha\Lambda L_N^2}$ [5].

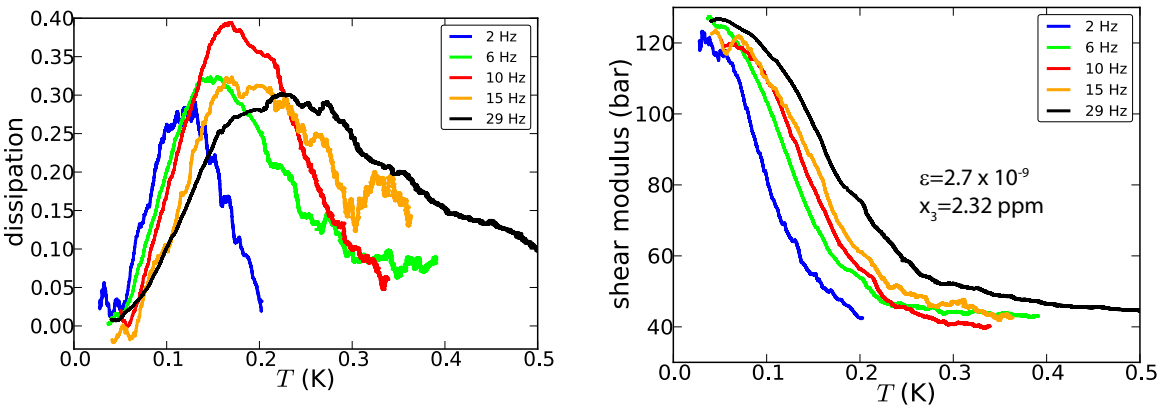


**Figure 2.** The dissipation and shear modulus measured on cooling at an rms driving strain of $2.7 \times 10^{-9}$ with the same crystal as in Fig. 1. The $^3$He concentration was 2.32 ppm.

Substituting $\tau = B_3 L_N^2/\pi^2 C$, since phonon damping is negligible, implies

$$f = f_\infty \exp(-nE_B/T) \tag{5}$$

where $f = \omega/2\pi$ and

$$f_\infty = \frac{\pi C\sqrt{1+\alpha\Lambda L_N^2}}{2B_0 x_3^n L_N^2} \tag{6}$$

The black solid line in Fig. 3 is a fit of Eq. 5 to the data from the 2.32 ppm crystal with best fit values $nE_B$ =0.73 K and $f_\infty$ = 757 Hz. Using Eq. 6 with $f_\infty$ = 757 Hz and the values $L_N = 158$ $\mu$m and $\Lambda = 4.1 \times 10^5/\mathrm{cm}^2$ determined above, we obtain $B_0 x_3^n = 3.3 \times 10^{-7}$ kg/sec m.

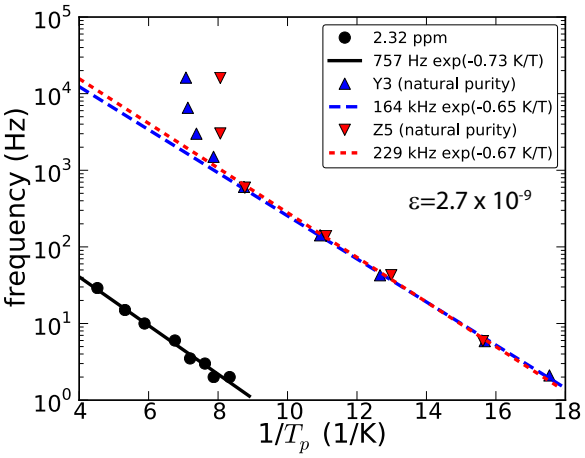


**Figure 3.** The black circles show $1/T_p$, the inverse temperature of the $Q^{-1}$ peak, measured at different driving frequencies (Fig. 2). These measurements were made at low driving strain $\epsilon = 2.7 \times 10^{-9}$. The black line is a fit of Eq. 5 to the data. The red and blue data points are measurements at the same driving strain on natural purity crystals studied in [3, 5] and the red and blue lines are corresponding fits of Eq. 5.

In order to determine the value of $n$, we use measurements on natural purity crystals from our previous work and the analysis procedure given above. The natural purity crystal Y3 studied by Haziot *et al.* [3] had $L_N = 88$ $\mu$m and $\Lambda = 5.5 \times 10^5/\mathrm{cm}^2$. Fefferman *et al.* [5] reported that natural purity crystal Z5 had $L_N = 96$ $\mu$m and $\Lambda = 7.9 \times 10^5/\mathrm{cm}^2$. The frequency dependence of $T_p$ for Y3 and Z5 and corresponding fits using Eq. 5 are shown in Figure 3. Using Eq. 6 we find that the values of $B_0 x_3^n$ for crystals Y3 and Z5 are respectively $3.8 \times 10^{-9}$ and $2.6 \times 10^{-9}$ kg/sec m, so that the respective ratios to the value of $B_0 x_3^n$ at 2.32 ppm are 0.012 and $7.9 \times 10^{-3}$.

The concentration of $^3$He in the natural purity helium from our supplier was $x_3 = 3.6 \times 10^{-8}$, which is 0.016 times that of our 2.32 ppm sample. Our natural purity helium had much less $^3$He than the natural purity helium of [13], in which $x_3 = 1.7 \times 10^{-7}$ was measured, demonstrating that $x_3$ is far from universal. It may vary by two orders of magnitude depending on the origin of the helium [14]. Under the assumption that $x_3$ of our supplier's helium has been constant over the last three years (we intend to verify this), our results are much more consistent with a linear dependence of the $^3$He damping coefficient on $^3$He concentration ($n = 1$) than with, e.g., a quadratic dependence. This implies that the slopes of the Arrhenius plots in [3, 5, 7] indeed give the binding energy, $E_B = 0.7$ K, as had been assumed in those works. Kim *et al.* [15] and Iwasa [16] made the estimates $E_B = 0.4$ and 0.2 K, respectively. These estimates would only be consistent with the damping measurements in the present work and in [3, 5, 7] if $n \approx 2$, but our preliminary results imply that this is not the case.

## Acknowledgments

We are grateful to P. Jean-Baptiste (LSCE, CEA, Saclay, France) for the measurement of the isotopic purity of our samples. This work was supported by grants from ERC (AdG 247258-SUPERSOLID) and from NSERC Canada.

## References

[1] Haziot A, Rojas X, Fefferman A D, Beamish J R and Balibar S 2013 *Phys. Rev. Lett.* **110**(3) 035301 URL http://link.aps.org/doi/10.1103/PhysRevLett.110.035301
[2] Haziot A, Fefferman A D, Beamish J R and Balibar S 2013 *Phys. Rev. B* **87**(6) 060509 URL http://link.aps.org/doi/10.1103/PhysRevB.87.060509
[3] Haziot A, Fefferman A D, Souris F, Beamish J R, Maris H J and Balibar S 2013 *Phys. Rev. B* **88**(1) 014106 URL http://link.aps.org/doi/10.1103/PhysRevB.88.014106
[4] Haziot A, Rojas X, Fefferman A D, Beamish J R and Balibar S 2013 *Phys. Rev. Lett.* **111**(11) 119602 URL http://link.aps.org/doi/10.1103/PhysRevLett.111.119602
[5] Fefferman A D, Souris F, Haziot A, Beamish J R and Balibar S 2014 *Phys. Rev. B* **89**(1) 014105 URL http://link.aps.org/doi/10.1103/PhysRevB.89.014105
[6] Granato A and Lucke K 1956 *J. Appl. Phys.* **27** 583
[7] Syshchenko O, Day J and Beamish J 2010 *Phys. Rev. Lett.* **104** 195301
[8] Hull D and Bacon D 2000 *Introduction to Dislocations* (Oxford, UK: Butterworth-Heinemann Elsevier)
[9] Hirth J and Lothe J 1964 *Theory of dislocations* (Malabar, Florida, USA: Krieger publishing company)
[10] Greywall D S 1977 *Phys. Rev. B* **16**(11) 5127–5128 URL http://link.aps.org/doi/10.1103/PhysRevB.16.5127
[11] Ninomiya T 1974 *J. Phys. Soc. Japan* **36** 399
[12] Ninomiya T 1984 *Scripta Metall. Mater.* **18** 669
[13] Vekhov Y, Mullin W and Hallock R 2013 arXiv:1311.4913v1
[14] Oxburgh E R, O'Nions R K and Hill R I 1986 *Nature* **324** 632
[15] Kim E, Xia J S, West J T, Lin X, Clark A C and Chan M H W 2008 *Phys. Rev. Lett.* **100**(6) 065301 URL http://link.aps.org/doi/10.1103/PhysRevLett.100.065301
[16] Iwasa I 2013 *J. Low Temp. Phys.* **171** 30